2016 IEEE International Conference on Advanced Intelligent Mechatronics (AIM)
Banff, Alberta, Canada, July 12–15, 2016

Development of a Robotic Finger with an Active Dual-mode Twisting Actuation and a Miniature Tendon Tension Sensor

Seok Hwan Jeong, Kyung-Soo Kim, Member, IEEE, and Soohyun Kim

Abstract— **A robot finger is developed with enhanced grasping force and speed using active dual-mode twisting actuation, which is a type of twisted string actuation. This actuation system has two twisting modes (Speed Mode and Force Mode) with different radii of the twisted string, and the twisting mode can be changed automatically. Therefore, the actuator operates like an automatic transmission having two transmission ratios, and the robot finger can generate a large grasping force or fast motion depending on the twisting mode. In addition, a miniature tendon tension sensor is developed and embedded in the fingertip for automatic mode change and grasping force control. A relation between the fingertip force and the tension of the tendon is derived by kinematic and kinetic analyses of the robot finger. The performance of the robotic finger and the tension sensor are verified by experimental results.**

I. Introduction

In the past several decades, there has been increasing interest in robot hands, with progress in manipulators and humanoid robots. The robot hand (or gripper) attached to the end of the manipulator plays a role as an end-effector, interacting with the external environment containing objects or humans. One of the most powerful and dexterous end-effectors is the human hand. It is able to generate a grasping force of up to approximately 400 N and 2290 degree/sec for flexion motion and complex motion using numerous muscles [1]. Therefore, many recent robot hands have imitated the function and structure of the human hand and tried to achieve human hand performance. The Shadow Dexterous Hand, which is one of the state-of-the-art robot hands, also imitates the human tendon mechanism as a driveline to implement multi degrees of freedom. Its pneumatic actuator behaves much like a biological muscle in generating high power [2]. The DLR Hand Arm system also uses a tendon as a driveline to generate a high degree of freedom [3]. As mentioned above, the tendon-driven mechanism gives the robot hand more freedom to move with a compact size. Although the mechanism is very advantageous for the robot hand, it cannot solve the problem caused by limited actuation power to achieve the human grasping force. To overcome this limitation, many actuators have been developed and adopted to the robot hand. For instance, shape memory alloys (SMAs) [4], super-coiled polymers (SCPs) [5], and electric motors [6] have been used in robot hands as actuators. However, these types of actuator have problems such as low energy efficiency, slow response time and low energy density. Pneumatic [7] or hydraulic actuators [8] have attracted attention as powerful actuators, but they generate loud engine noise and need a large space for their massive compressors. Therefore, it is still difficult for actuators to achieve the human muscle power, and many studies are being carried out to develop a new type of actuator.

For this reason, we focused on the actuation mechanism rather than the performance of the actuator itself. Among the various actuation mechanisms, twisted string actuation (TSA) was suggested in [9, 10]. This system utilizes a linear contraction force by a twisted string, producing an extremely high transmission ratio and generating a large contraction force. A rotary actuator like an electric motor rotates a single string or string pair without additional mechanical parts such as gears or screws. The twisted string plays a role as not only an actuator but also a driveline at the same time. Therefore, TSA is very promising for compact multi-joint robots such as a robot hand, utilizing space efficiently. In [10], a robot hand uses TSA as a driving mechanism. However, a major problem in this type of mechanism is the fixed transmission ratio and slow contraction speed. To overcome these drawbacks, a variable twisting mechanism, called dual-mode twisting actuation (passive dual-mode), was suggested in [11]. It has dual twisting parts that have different twisted radii, but the twisting modes are only changed by an external force. To make the passive transmission process automatic, we added a miniature motor, which plays a role as a clutch, to the dual-mode system in [12]. By using this mechanism, an automatic transmission system can be realized. We named it active dual-mode twisting actuation (active dual-mode).

In this paper, we newly suggest a robot finger using active dual-mode twisting actuation to achieve the human hand performance. In addition, a miniature tendon tension sensor is introduced for grasping force control.

This paper is organized as follows. Section II is devoted to an introduction of the driving mechanism. In Section III, the design of the robot finger is analyzed. In Section IV, experiments are performed to verify the performance of the proposed robot finger. Finally, concluding remarks follow in Section V.

II. Introduction of Driving Mechanism

A. Active dual-mode twisting actuation

The active dual-mode consists of a main motor, clutch motor, shaft, clutch gear, a pair of strings, twisted coupler 1 (TC1) and twisted coupler 2 (TC2), as shown in Fig. 1 (a). This mechanism has two twisting modes. As shown in Fig. 1

This work was supported by the Technology Innovation Program (10051330) funded By the Ministry of Trade, industry & Energy(MI, Korea).

Seok Hwan Jeong is with the Mechanical Engineering Department, Korea Advanced Institute of Science and Technology (KAIST), Daejeon, 305-701, Republic of Korea (e-mail: astroidbelt@kaist.ac.kr)

Kyung-Soo Kim is with the Mechanical Engineering Department, Korea Advanced Institute of Science and Technology (KAIST), Daejeon, 305-701, Republic of Korea (e-mail: kyungsookim@kaist.ac.kr).

Kyung-Soo Kim is with the Mechanical Engineering Department, Korea Advanced Institute of Science and Technology (KAIST), Daejeon, 305-701, Republic of Korea (e-mail: soohyun@kaist.ac.kr).

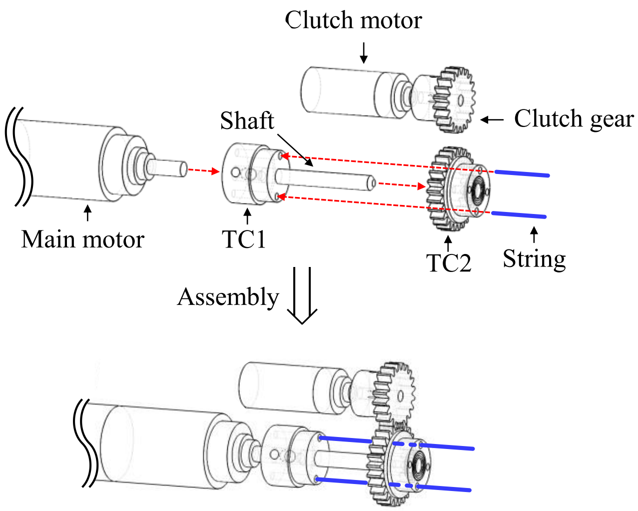

(a)

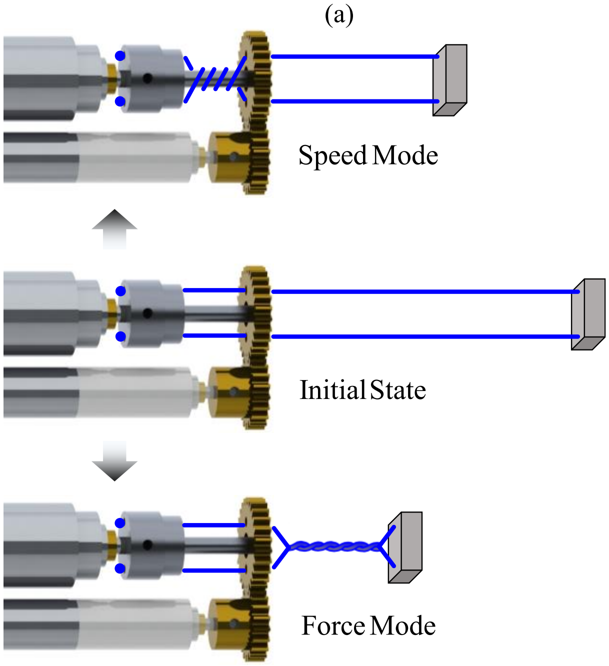

(b)

Figure 1. Active dual-mode actuation. (a) Mechanical parts. (b) Twisting modes (Speed Mode – Initial state – Force Mode)

(b), if the main motor rotates and the clutch motor is fixed, the pair of strings is wound around the shaft, having a large twisted radius. This twisting mode, which is called Speed Mode, generates a fast contraction speed from the initial state. Conversely, if the main motor and clutch motor rotate simultaneously, the strings are twisted themselves. This twisting mode is called Force Mode and generates a large contraction force. Due to the different twisted radius in each mode, different transmission ratios can be implemented. Mode switching between Speed Mode and Force Mode can be implemented through control of the clutch motor. Suppose that we want to change the twisting mode to Force Mode from Speed Mode. The clutch motor rotates the TC 2 to twist the strings themselves, generating Force Mode. At the same time, the strings, which are twisted around the shaft, are unwound by the rotation of the main motor to remove the effect of the Speed Mode. Therefore, active dual-mode works like an automatic transmission system. The performance was verified in [12].

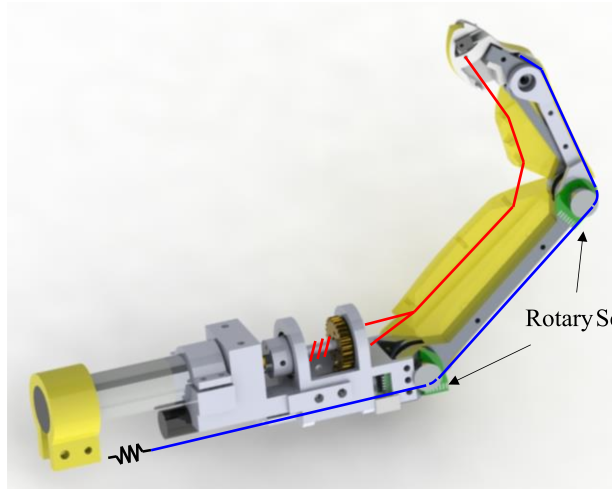

(a)

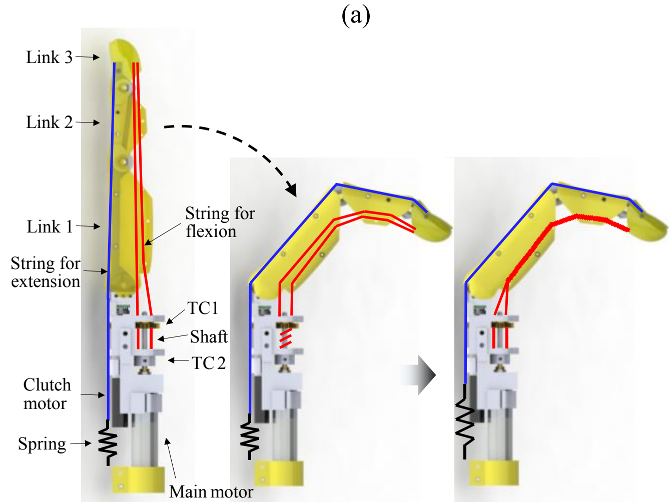

(b)

Figure 2. Developed robot finger. (a) Overall design of robot finger (b) Driving mechanism (red string for flexion, blue string and spring for extension)

B. Design and Mechanism of the Robot Finger

To apply the active dual-mode actuation to a robot finger as an actuator, we designed a robot finger driven by a tendon mechanism. Fig. 2 shows the overall design and driving mechanism of the developed robot finger. It consists of three links (link 1, link 2 and link 3), where link 2 and link 3 are mechanically coupled by a 4-bar linkage structure like that of a human. The magnetic rotary encoders (AS5045) are embedded in the first and second joints, and they measure rotation angles.

The flexion and extension motions are driven by the contraction force of the strings, which are tied at link 3, and each contraction force is from the active dual-mode and spring. Because the robot finger has one more degree of freedom than the actuator, it operates as an under-actuated system. When the robot finger needs a fast grasping motion (e.g., catching an object), the active dual-mode operates in Speed Mode. Then, when the robot finger needs a large grasping force (e.g., a tight grip), it generates the Force Mode, twisting through mode transition control, as shown in Fig. 2 (b). Therefore, the robot

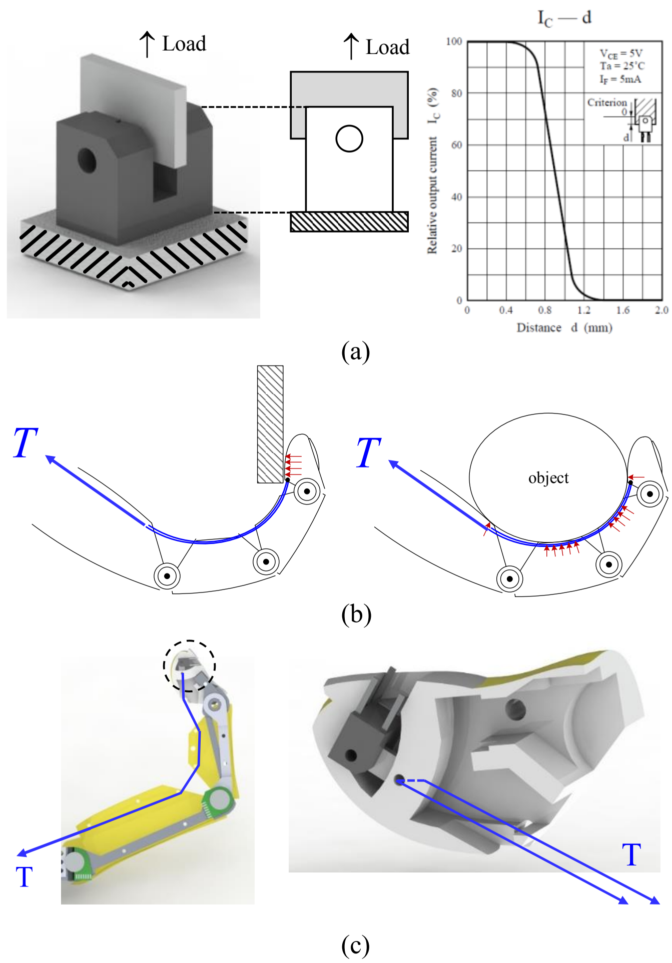

Figure 3. (a) Principle of force sensor using photo interrupter (left) and current-distance graph of photo interrupter (CAN-1311K) (right). (b) Point contact (left) and surface contact (right). (c) Developed tendon tension sensor

can have two different transmission ratios depending on the situations, and it has a wide force-velocity operating area.

C. *Tendon tension sensor*

A force sensor is a prerequisite for the force control of the robot finger. Furthermore, force information is necessary for the active mode change and is used as a threshold of the mode change in active dual-mode.

Various force sensors have been developed using the principles of strain gage [13], conductive film [14], piezoelectric resistor [15], capacitor [16] and optical fiber [17]. Although these sensors have good sensitivity and high-resolution arrays, they require delicate efforts to manufacture and sophisticated installation and calibration processes that makes them very expansive. To overcome these problems, a photo interrupter based force sensor (PFS) was developed in [18]. The PFS consists of a miniature photo interrupter and elastic slit, as shown in Fig. 3 (a). Once an external load is applied to the elastic slit, which is located in the light path, deformation occurs, and the amount of light passing through the slit is changed. By measuring the variation of voltage from the sensor, we can estimate the exerted force. By using the PFS, the force sensor can be simply miniaturized and manufactured inexpensively without complicated processing.

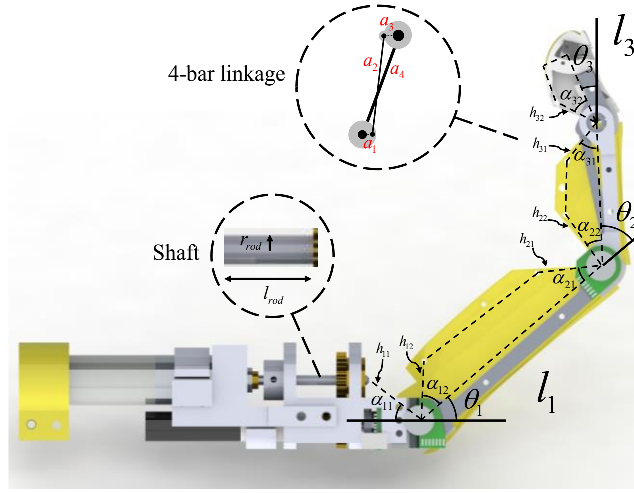

Figure 4. Structure of the developed robot finger

TABLE I
SPECIFICATIONS OF THE EXPERIMENT PARAMETERS

Items	Specification
Link (mm)	$l_1 = 47.5,\ l_2 = 28.5,\ l_3 = 10$
h_{j1} (mm)	$h_{11} = 13.4,\ h_{21} = 12.78,\ h_{31} = 9.67$
h_{j2} (mm)	$h_{12} = 11.84,\ h_{22} = 12.41,\ h_{32} = 8.87$
4-bar link length (mm)	$a_1 = 2.5,\ a_2 = 26.2,\ a_3 = 3,\ a_4 = l_2 = 28.5$
α_{j1} (degree)	$a_{11} = 36.66,\ \alpha_{21} = 33.8,\ \alpha_{31} = 39.11$
α_{j2} (degree)	$a_{12} = 45,\ \alpha_{22} = 33.12,\ \alpha_{32} = 38.53$
Length of Shaft (mm)	$l_{rod} = 7.7$
Length of radius (mm)	$r_{rod} = 1$

In robot hand applications, a tactile sensor is commonly used as a force sensor and installed in a finger-tip. However, sensors should cover all surfaces of the finger because objects are not always in contact with a finger-tip, as shown in Fig. 3 (b). This increases the number of sensors required and results in expensive installation costs. However, if we measure only the tension applied to the tendon, it can cover all grasping cases, including point contact and surface contact, with only one force sensor, as shown in Fig. 3 (b). For the above reasons, we developed a photo interrupter (CAN-1311K)-based miniature tendon tension sensor, as shown in Fig. 3 (c). The sensor is embedded in a finger-tip, and an elastic slit is made of 3-D printed material (Stratasys VeroWhitePlus RGD835). Because this type of force-sensing mechanism does not need numerous tactile sensors, the whole system can be compact and cost-effective.

III. ANALYSIS OF THE ROBOT FINGER

In this section, the relationship between the bending angles of each joint and contracted length of string is derived by a kinematic analysis of the robot finger. In addition, the finger-tip force is estimated from the tension of the tendon by kinetic analysis.

A. *Kinematic Analysis of a Robot finger*

The parameters of the developed robot finger are summarized in Table I, and the kinematic structure of the robot finger is shown in Fig. 4. The 4-bar linkage connecting joint 2 and joint 3 is designed to imitate human finger motion, which is fully extended in the open-handed posture and bent in the grasping posture. Therefore, a finger has two degrees of freedom. By contracting the string passing through the inside

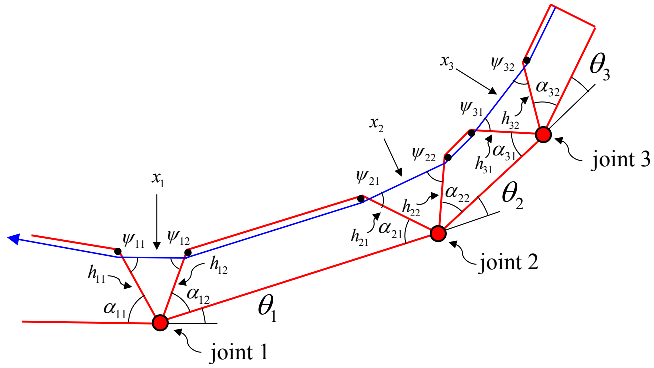

Figure 5. Geometry of the robot finger

of the finger, a grasping motion is generated. By using the law of cosines, the relation between the contracted string length ΔX and the joint angles θ_k is derived as

$$\begin{aligned}\Delta X &= X_O - X = \Delta x_1 + \Delta x_2 + \Delta x_3 \\ &= \sum_{j=1}^{3}\sqrt{h_{j1}^2 + h_{j2}^2 + 2h_{j1}h_{j2}\cos(\alpha_{n1}+\alpha_{n2})} \\ &\quad -\sum_{k=1}^{3}\sqrt{h_{k1}^2 + h_{k2}^2 + 2h_{k1}h_{k2}\cos(\alpha_{k1}+\alpha_{k2}+\theta_k)}\end{aligned} \quad (1)$$

where Δx_k is the length of one side of the triangle created by the string and each segment of the finger, as shown in Fig. 5.

Angle ψ also can be derived by using the law of sines, and it is expressed as follows:

$$\begin{aligned}\psi_{n1} &= \sin^{-1}\left(\frac{\mathrm{h}_{n2}\sin(\alpha_{n1}+\alpha_{n2}+\theta_n)}{\sqrt{h_{n1}{}^2 + h_{n2}{}^2 + 2h_{n1}h_{n2}\cos(\alpha_{n1}+\alpha_{n2}+\theta_n)}}\right) \\ \psi_{n2} &= \sin^{-1}\left(\frac{\mathrm{h}_{n1}\sin(\alpha_{n1}+\alpha_{n2}+\theta_n)}{\sqrt{h_{n1}{}^2 + h_{n2}{}^2 + 2h_{n1}h_{n2}\cos(\alpha_{n1}+\alpha_{n2}+\theta_n)}}\right)\end{aligned} \quad (2)$$

Note that ψ is needed for the kinetic analysis of the robot finger.

B. *Kinematic Analysis of a Robot finger*

The finger-tip force F and string tension T are mechanically coupled, and F can be estimated by measuring T. Therefore, a kinetic analysis of the robot finger is required to obtain the relation between F and T. Once an external force F is exerted on the finger-tip, the internal force f_k and torque τ_k at the each joint k are expressed as shown in Fig. 6 (a). f_x and f_y are the horizontal and vertical components of F. Then, τ_k can be expressed as follows:

$$\begin{aligned}\tau_1 &= \vec{r_{11}}\times\vec{T_1} - \vec{r_{12}}\times\vec{T_2} - \vec{r_{13}}\times\vec{f_2} \\ \tau_2 &= \vec{r_{21}}\times\vec{T_2} - \vec{r_{22}}\times\vec{T_3} - \vec{r_{23}}\times\vec{f_3} \\ \tau_3 &= \vec{r_{31}}\times\vec{T_1} + \vec{r_{33}}\times F\end{aligned} \quad (3)$$

Then, the sum of $\vec{T}$ and $\vec{F}$ is zero in each segment of the finger due to the static equilibrium state, and it is expressed as follows:

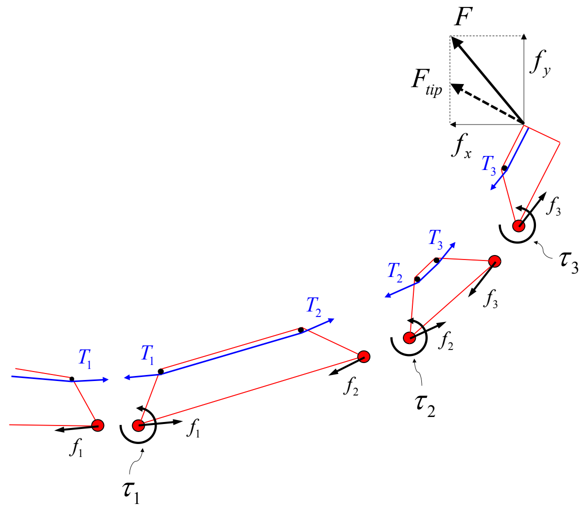

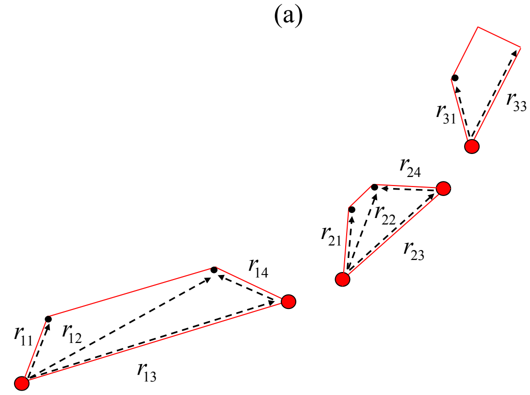

Figure 6. (a) External and internal forces and torque of the each segment of finger. (b) Geometry of the robot finger.

$$\begin{aligned}\vec{T_1} - \vec{T_2} + \vec{f_1} - \vec{f_2} &= 0 \\ \vec{T_2} - \vec{T_3} + \vec{f_2} - \vec{f_3} &= 0 \\ \vec{T_3} + \vec{f_3} + \vec{F} &= 0\end{aligned} \quad (4)$$

Then, the joint torque and fingertip force can be described by

$$\begin{bmatrix}\tau_1 & \tau_2 & \tau_3\end{bmatrix}^T = J^T \cdot \begin{bmatrix} f_x \\ f_y \end{bmatrix} \quad (5)$$

where J is the Jacobian matrix. By substituting (3) and (4) for (5), the fingertip force can be derived as follows:

$$\begin{bmatrix} f_x \\ f_y \end{bmatrix} = \left(\left(J^T - B\right)^T \left(J^T - B\right)\right)^{-1} \left(J^T - B\right)^T A \cdot T \quad (6)$$

where

$$A = \begin{bmatrix} h_{12}\sin(\psi_{12}) - h_{21}\sin(\psi_{21}) \\ h_{22}\sin(\psi_{22}) - h_{31}\sin(\psi_{31}) \\ h_{32}\sin(\psi_{32}) \end{bmatrix}$$

$$B = \begin{bmatrix} -l_1\sin(\theta_1) & l_1\cos(\theta_1) \\ -l_2\sin(\theta_1+\theta_2) & l_2\cos(\theta_1+\theta_2) \\ -l_3\sin(\theta_1+\theta_2+\theta_3) & l_3\cos(\theta_1+\theta_2+\theta_3) \end{bmatrix}$$

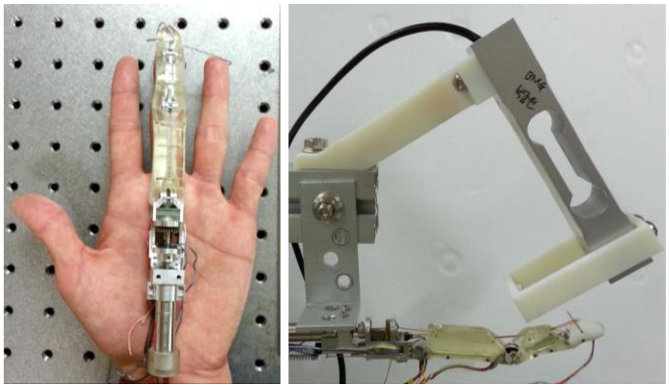

Figure 7. Developed robot finger (left) and experimental setup (right).

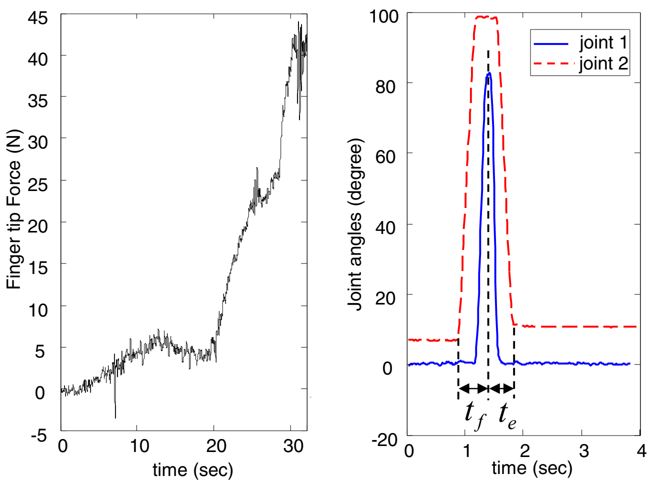

Figure 8. Experimental result of the fingertip force (left) and joint angles (right)

Then, F_{tip}, which is the force component perpendicular to the fingertip, is derived as follows:

$$F_{tip} = \begin{bmatrix} -\sin(\theta_1+\theta_2+\theta_3) & \cos(\theta_1+\theta_2+\theta_3) \end{bmatrix} \begin{bmatrix} f_x \\ f_y \end{bmatrix} \quad (7)$$
$$= G(\theta_1,\theta_2,\theta_3)\cdot T$$

As a result, we can estimate F_{tip} by using hte joint angles and the tension of the string. Therefore, delicate force control and twisting mode transition control according to the external force are possible by using F_{tip}.

IV. Experiments

A. Performance of the robot finger

To verify the performance of the active dual-mode in the robot finger, we measured joint angles θ_1 and θ_2 and the fingertip force F_{tip} in both Speed Mode and Force Mode. The joint angles and fingertip force are obtained by a magnetic rotary encoder and load cell (BCL-30L), respectively, as shown in Fig. 7. The experimental result is shown in Fig. 8. The maximum fingertip force reaches up to 44.06 N. The flexion time t_f and extension time t_e are measured as 0.54 sec and 0.43 sec, respectively, with average angular speeds of 316 degree/sec and 404 degree/sec.

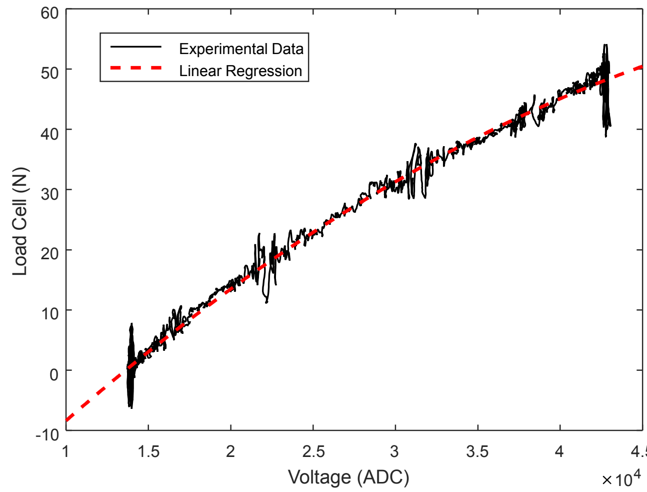

(a)

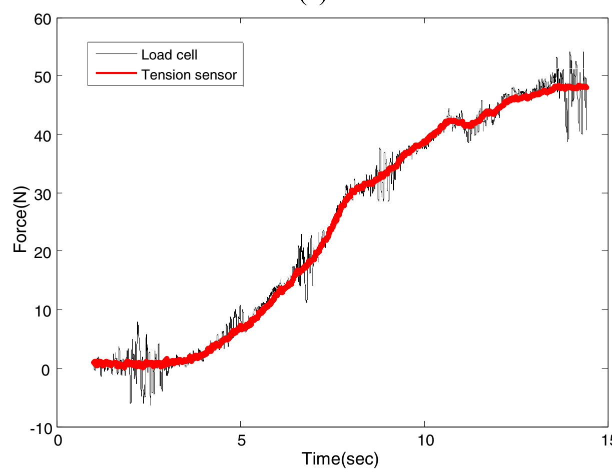

(b)

Figure 9. Experimental result of the tendon tension sensor. (a) Linear regression for calibration. (b) Actual tension and calibrated tension

B. Calibration of Tendon Tension Sensor

To estimate F_{tip}, we need tension information from the developed tension sensor. Therefore, a calibration process is required to obtain the exact tension value. The actual tension value is measured by a load cell, and the voltage V from the photo interrupter is also measured; they are connected through the string during the calibration process. From the experimental result, the actual tension and consequent voltage are obtained, as shown in Fig. 9 (a), and the relation can be expressed as a 2nd-degree polynomial equation by linear regression as follows:

$$T = -2.019\cdot 10^{-8} V^2 + 0.00279V - 34.269 \quad (8)$$

Using the (8), the actual tension can be estimated by measuring V as shown in Fig. 9 (b).

C. Estimation of the Fingertip Force

According to the above kinetic analysis of the robot finger, we can estimate the fingertip force F_{tip} by using (7). The finger position is fixed at specific joint angles, and the actual fingertip force is measured by a load cell to compare with the estimated fingertip force F_{tip}. The experimental result is as shown in Fig. 10. The estimated fingertip force is close to the

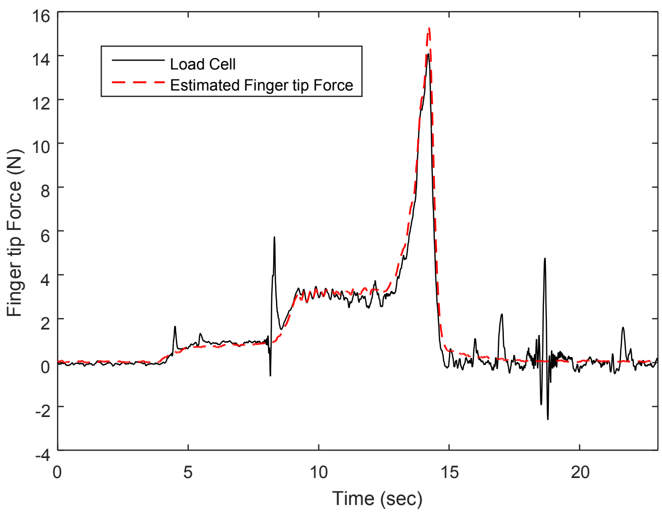

Figure 10. Actual fingertip force and estimated fingertip force

actual fingertip force, with a 0.62 N root mean square (RMS) error.

V. Conclusions

In this paper, we developed a robot finger using an active dual-mode twisting actuator and a tendon tension sensor. By the powerful contraction force of the twisted string mechanism, the fingertip force can reach up to 44.06 N in Force Mode, and it takes only 0.54 sec to make a grasping motion in Speed Mode by changing the twisted radius. In comparison with the built-in type prosthetic robot hands in [19], the developed robot finger shows the best performance in terms of grasping force and speed. Due to the active dual-mode, the robot finger can have a wide operating area, and we expect that it can be used in a variety of situations.

Furthermore, we developed a photo interrupter based miniature tension sensor. The sensor measures the tension of the string, so the fingertip force can be estimated without a tactile sensor. Using this tendon structure, various grasping situations can be controlled including point contact (fingertip contact) and surface contact (covering object) without a large number of tactile sensors. This results in a cost reduction and simplified robot system. The experimental result for the estimation of the fingertip force shows that the developed tendon-based system works effectively.

Future works will be focusing mode transition algorithm and force control to interact external environment.

References

[1] R. F. Weir and J. W. Sensinger, "Design of artificial arms and hands for prosthetic applications," ed: McGraw Hill, New York, 2003, pp. 32.1-32.61.

[2] A. Kochan, "Shadow delivers first hand," *Industrial robot: an international journal,* vol. 32, pp. 15-16, 2005.

[3] M. Grebenstein, A. Albu-Schäffer, T. Bahls, M. Chalon, O. Eiberger, W. Friedl, *et al.*, "The DLR hand arm system," in *Robotics and Automation (ICRA), 2011 IEEE International Conference on*, 2011, pp. 3175-3182.

[4] T. Maeno and T. Hino, "Miniature five-fingered robot hand driven by shape memory alloy actuators," in *Proceedings of the 12th IASTED International Conference on Robotics and Applications*, 2006, pp. 174-179.

[5] M. C. Yip and G. Niemeyer, "High-performance robotic muscles from conductive nylon sewing thread," in *Robotics and Automation (ICRA), 2015 IEEE International Conference on*, 2015, pp. 2313-2318.

[6] C. Lovchik and M. A. Diftler, "The robonaut hand: A dexterous robot hand for space," in *Robotics and Automation, 1999. Proceedings. 1999 IEEE International Conference on*, 1999, pp. 907-912.

[7] N. Tsujiuchi, T. Koizumi, S. Nishino, H. Komatsubara, T. Kudawara, and M. Hirano, "Development of pneumatic robot hand and construction of master-slave system," *Journal of system design and dynamics,* vol. 2, pp. 1306-1315, 2008.

[8] M. Raibert, K. Blankespoor, G. Nelson, R. Playter, and T. Team, "Bigdog, the rough-terrain quadruped robot," in *Proceedings of the 17th World Congress*, 2008, pp. 10822-10825.

[9] M. Shoham, "Twisting wire actuator," *Journal of Mechanical Design,* vol. 127, pp. 441-445, 2005.

[10] T. Würtz, C. May, B. Holz, C. Natale, G. Palli, and C. Melchiorri, "The twisted string actuation system: Modeling and control," in *Advanced Intelligent Mechatronics (AIM), 2010 IEEE/ASME International Conference on*, 2010, pp. 1215-1220.

[11] Y. J. Shin, H. J. Lee, K.-S. Kim, and S. Kim, "A robot finger design using a dual-mode twisting mechanism to achieve high-speed motion and large grasping force," *Robotics, IEEE Transactions on,* vol. 28, pp. 1398-1405, 2012.

[12] S. H. jeong, Y. J. Shin, K.-S. Kim, and S. Kim, "Dual-Mode Twisting Actuation Mechanism with an Active Clutch for Active Mode-Change and Simple Relaxation Process," in *IEEE/RSJ International Conference on Intelligent Robots and Systems*, 2015.

[13] E.-S. Hwang, J.-h. Seo, and Y.-J. Kim, "A polymer-based flexible tactile sensor for both normal and shear load detections and its application for robotics," *Microelectromechanical Systems, Journal of,* vol. 16, pp. 556-563, 2007.

[14] Z. Del Prete, L. Monteleone, and R. Steindler, "A novel pressure array sensor based on contact resistance variation: Metrological properties," *Review of Scientific Instruments,* vol. 72, pp. 1548-1553, 2001.

[15] G. Buscher, M. Meier, G. Walck, R. Haschke, and H. J. Ritter, "Augmenting curved robot surfaces with soft tactile skin," in *Intelligent Robots and Systems (IROS), 2015 IEEE/RSJ International Conference on*, 2015, pp. 1514-1519.

[16] H.-K. Lee, J. Chung, S.-I. Chang, and E. Yoon, "Normal and shear force measurement using a flexible polymer tactile sensor with embedded multiple capacitors," *Microelectromechanical Systems, Journal of,* vol. 17, pp. 934-942, 2008.

[17] L. Jiang, K. Low, J. Costa, R. J. Black, and Y.-L. Park, "Fiber optically sensorized multi-fingered robotic hand," in *Intelligent Robots and Systems (IROS), 2015 IEEE/RSJ International Conference on*, 2015, pp. 1763-1768.

[18] J.-C. Kim, J. Lee, K.-S. Kim, and S. Kim, "A tri-axial force sensor based on light intensity modulation for detecting ground reaction force," in *Robotics (ISR), 2013 44th International Symposium on*, 2013, pp. 1-5.

[19] J. T. Belter and A. M. Dollar, "Performance characteristics of anthropomorphic prosthetic hands," in *IEEE International Conference on Rehabilitation Robotics*, 2011, pp. 921-927.